Biochimica et Biophysica Acta 1807 (2011) 1295–1304

Contents lists available at ScienceDirect

Biochimica et Biophysica Acta

journal homepage: www.elsevier.com/locate/bbabio

Radical formation in cytochrome *c* oxidase ☆

Michelle A. Yu [a,1], Tsuyoshi Egawa [a,1], Kyoko Shinzawa-Itoh [b], Shinya Yoshikawa [b], Syun-Ru Yeh [a], Denis L. Rousseau [a,*], Gary J. Gerfen [a,**]

[a] Department of Physiology and Biophysics, Albert Einstein College of Medicine, 1300 Morris Park Ave., Bronx, NY 10461, USA
[b] Department of Life Science, University of Hyogo, 3-2-1 Kouto, Kamigori, Ako, Hyogo 678-1297, Japan

ARTICLE INFO

Article history:
Received 19 April 2011
Received in revised form 14 June 2011
Accepted 15 June 2011
Available online 22 June 2011

Keywords:
Bioenergetics
Electron paramagnetic resonance
Radicals
Proton translocation
Peroxyl

ABSTRACT

The formation of radicals in bovine cytochrome *c* oxidase (bCcO), during the O_2 redox chemistry and proton translocation, is an unresolved controversial issue. To determine if radicals are formed in the catalytic reaction of bCcO under single turnover conditions, the reaction of O_2 with the enzyme, reduced by either ascorbate or dithionite, was initiated in a custom-built rapid freeze quenching (RFQ) device and the products were trapped at 77 K at reaction times ranging from 50 μs to 6 ms. Additional samples were hand mixed to attain multiple turnover conditions and quenched with a reaction time of minutes. X-band (9 GHz) continuous wave electron paramagnetic resonance (CW-EPR) spectra of the reaction products revealed the formation of a narrow radical with both reductants. D-band (130 GHz) pulsed EPR spectra allowed for the determination of the *g*-tensor principal values and revealed that when ascorbate was used as the reductant the dominant radical species was localized on the ascorbyl moiety, and when dithionite was used as the reductant the radical was the $SO_2^{\bullet -}$ ion. When the contributions from the reductants are subtracted from the spectra, no evidence for a protein-based radical could be found in the reaction of O_2 with reduced bCcO. As a surrogate for radicals formed on reaction intermediates, the reaction of hydrogen peroxide (H_2O_2) with oxidized bCcO was studied at pH 6 and pH 8 by trapping the products at 50 μs with the RFQ device to determine the initial reaction events. For comparison, radicals formed after several minutes of incubation were also examined, and X-band and D-band analysis led to the identification of radicals on Tyr-244 and Tyr-129. In the RFQ measurements, a peroxyl (R–O–O•) species was formed, presumably by the reaction between O_2 and an amino acid-based radical. It is postulated that Tyr-129 may play a central role as a proton loading site during proton translocation by ejecting a proton upon formation of the radical species and then becoming reprotonated during its reduction via a chain of three water molecules originating from the region of the propionate groups of heme a_3. This article is part of a Special Issue entitled: "Allosteric cooperativity in respiratory proteins".

© 2011 Published by Elsevier B.V.

1. Introduction

Cytochrome *c* oxidase (CcO) is a member of the heme-copper oxygen reductase superfamily, which encompasses the membrane-bound terminal enzymes in the electron transfer chain in organisms that utilize oxygen. These membrane-bound enzymes catalyze the 4-electron reduction of O_2 to two water molecules and use the free energy generated to pump four protons across the membrane in which they are located [1–3]. Four additional protons are consumed for the reduction of molecular oxygen to water resulting in the overall reaction:

$$4e^- + 8H^+_{in} + O_2 \rightarrow 2H_2O + 4H^+_{out} \quad (1)$$

In eukaryotic species, such as bovine CcO (bCcO), in which the enzyme is located in the inner mitochondrial membrane, a two-atom copper center (Cu_A) accepts electrons from cytochrome *c* (Cyt *c*) and transfers them via a low-spin heme group (heme *a*) to a heme a_3–Cu_B binuclear center at which the four-electron reduction of oxygen to water takes place (Fig. 1). In the reduced state, heme a_3 is 5-coordinate with a histidine (His-376) axial ligand and Cu_B is coordinated by three histidine residues (His-240, 290 and 291—bCcO numbering is used throughout unless otherwise noted).

The O_2 reaction chemistry has been heavily studied and key intermediates have been identified [1,4–8] (Fig. 2). However, the formation of amino acid radicals and their roles during the oxygen reaction has not been delineated and remains a controversial issue [9]. Putative radical formation resulting from donation of an electron from

Abbreviations: PdCcO and bCcO, the aa_3 cytochrome *c* oxidases from *Paracoccus denitrificans* and bovine, respectively; Cu_A, the binuclear copper site in oxygen reductases; Cu_B, the copper atom which is part of the binuclear catalytic site in oxygen reductases; EPR, electron paramagnetic resonance; RFQ, rapid freeze quench

☆ This article is part of a Special Issue entitled: "Allosteric cooperativity in respiratory proteins".

* Corresponding author. Tel.: +1 718 430 4264.
** Corresponding author. Tel.: +1 718 430 2631.
E-mail addresses: denis.rousseau@einstein.yu.edu (D.L. Rousseau), gary.gerfen@einstein.yu.edu (G.J. Gerfen).

[1] These authors contributed equally to this project.

0005-2728/$ – see front matter © 2011 Published by Elsevier B.V.
doi:10.1016/j.bbabio.2011.06.012

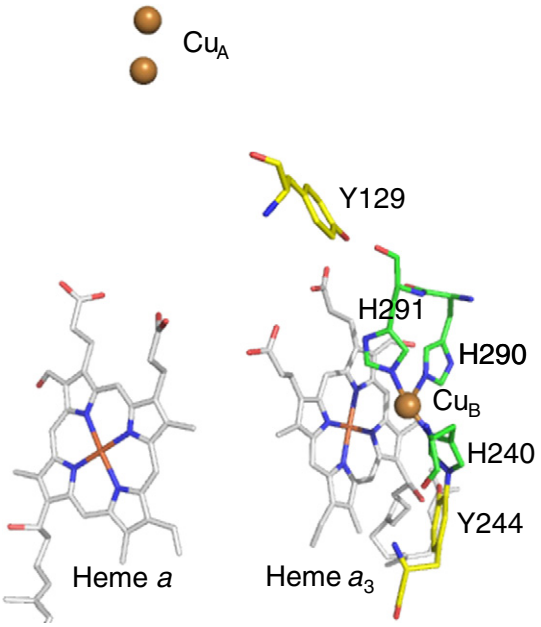

Fig. 1. The metal redox centers in cytochrome *c* oxidase (PDB ID: 3EHB). The heme a_3 and Cu_B, which are separated by ~5 Å, form a binuclear center at which the reduction of oxygen takes place. The figure was made with PyMol Molecular Graphics Software (Delano Scientific, LLC).

an amino acid residue to the binuclear center during oxygen reduction may be essential for rapidly cleaving the O–O bond in the formation of a "**P**" intermediate (**P_M** in Fig. 2) thereby preventing the release of reactive oxygen species; radicals have also been postulated to play a role in proton translocation [10,11]. The cleavage of the O–O bond with the concomitant formation of an OH^- ion and a ferryl state on heme a_3 requires 4 electrons. Starting with the reduced binuclear center, two electrons originate from the oxidation of the heme a_3 iron from Fe^{2+} to Fe^{4+} and one comes from the oxidation of Cu_B from Cu^{1+} to Cu^{2+}. The fourth electron can come from a reduced heme *a* center or from an amino acid residue. In the mixed valence (MV) enzyme, in which only the two metals in the binuclear site are reduced, while the others are oxidized, the fourth electron needed to cleave the O–O bond must come from an amino acid. It is widely believed that the "extra" electron originates from Tyr-244, the residue that is covalently linked to His-240, one of the Cu_B ligands [1]. Support for this assignment was made by radioactive iodide labeling followed by peptide mapping studies of the oxygen reaction with the MV oxidase carried out by Babcock and coworkers in which Tyr-244 became labeled, indicating the formation of a radical on this residue [12]. More recently other workers have reported radical formation on other residues during catalytic turnover [11,13].

In this paper, we summarize the prior reports of radical formation in heme-copper oxygen reductases. In addition, we define the conditions under which spurious radical formation can take place, and we report the identification of new radicals formed in the reaction of hydrogen peroxide with fully oxidized bC*c*O. From these observations a new center that can serve as a proton loading site during the catalytic reaction is suggested.

2. Materials and methods

The bC*c*O samples, isolated from bovine heart tissue, used in these measurements were prepared by two different methods. Some were prepared according to the protocol developed by Yoshikawa and coworkers [14]. Others were prepared from crystallization quality enzyme, by crystallizing the enzyme into microcrystals, collecting and then resolubilizing the crystals for the experiments. No qualitative differences between the two types of enzyme were observed. The enzyme concentrations were calculated using an extinction coefficient of 33.6 $mM^{-1}\,cm^{-1}$ for the fully-reduced C*c*O at 604 nm minus the oxidized enzyme at 630 nm [15].

Natural abundance L-ascorbic acid was obtained from Fisher Scientific, Waltham, MA. Isotopically labeled L-ascorbic acid was obtained from Omicron Biochemicals, South Bend, IN. A 1 M stock solution of ascorbate was prepared in degassed 0.2 M sodium phosphate buffer at pH 7.4 and the pH was adjusted with NaOH. A final concentration of 10 mM ascorbate was added to degassed bC*c*O and incubated with 0.5 μM Cyt *c* as the electron carrier. Sodium dithionite was obtained from Sigma-Aldrich, St. Louis, MO. A 1 M stock solution of dithionite was prepared in degassed 0.2 M sodium phosphate buffer at pH 7.4. A final concentration of 6 mM dithionite was added to degassed bC*c*O without Cyt *c*. 30% w/v hydrogen peroxide (Sigma-Aldrich, St. Louis, MO) was diluted in buffer, purged on ice for the anaerobic samples, and used within four hours. To make anaerobic samples the solutions were first purged with argon gas and then D-glucose (500 mM) and glucose oxidase (1.3 mg/ml) were added to remove any residual oxygen prior to the experiments.

Rapid freeze-quench (RFQ) is a novel technology used to trap transient radicals formed at room temperature for spectroscopic characterization at low temperature. RFQ samples were prepared using a custom-built device described previously [16,17]. For the reactions of O_2 with the fully reduced enzyme, resting bC*c*O was

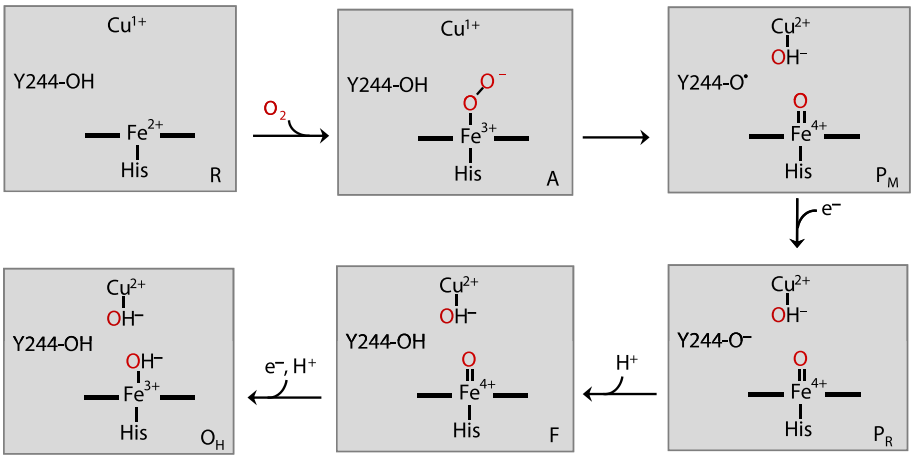

Fig. 2. Schematic sequence for the reaction of O_2 with cytochrome *c* oxidase. In general, the ligands on Cu_B have not been unequivocally determined. Thus, the addition of a proton in going from **P_R** to **F** could reside on either on Tyr-244, as indicated or on Cu_B.

reduced with either ascorbate or dithionite in a gas-tight syringe and mixed with oxygenated buffer in another gas-tight syringe at room temperature. For the reactions of H_2O_2 with the oxidized enzyme the resting bC*c*O in one gas-tight syringe was mixed with buffered H_2O_2 in another gas-tight syringe. To assure that the reaction could occur on the fast time scale and build up a population sufficient for EPR detection, a large excess of H_2O_2 was used. Samples were freeze-quenched on a timescale of 50 μs to 6 ms. The frozen powder was packed into 4-mm O.D. (X-band) or 0.55 mm O.D. (D-band) precision-bore quartz EPR tubes immersed in liquid nitrogen. Hand-quenched samples were prepared in similar EPR tubes and frozen in liquid nitrogen on the timescale of minutes.

X-band (9 GHz) measurements were made on a Varian E-line spectrometer. A finger dewar filled with liquid nitrogen and inserted into the EPR cavity maintained the sample at 77 K. Experimental conditions were: modulation amplitude, 3.2 G; microwave power, 1.0 or 0.3 mW; receiver gain, 2.5×10^4; microwave frequency, 9.1 GHz. The field was calibrated using Mn doped in MgO.

D-band (130 GHz) measurements were made on a spectrometer assembled at Albert Einstein College of Medicine, described by Gerfen and co-workers [18,19]. Hahn echo, field swept spectra were obtained with the following parameters: temperature, 7 K; repetition rate, 30 Hz; 30 averages per point; 90° pulse, 50 ns; time τ between pulses, 130 ns.

3. Results and discussion

Electron paramagnetic resonance (EPR) is a very powerful technique for characterizing radicals formed in the reactions of heme-copper oxidases and identifying the residue on which these radical form (for an excellent review see [20]). In addition, the oxidation state of the metals in the enzyme can be assessed based on the EPR spectra of the heme groups and the copper centers. In the Supplementary material, we present the general characteristics of the EPR spectra from the iron and the copper centers.

3.1. Search for spectroscopic evidence of radicals formed during the catalytic reaction

During the catalytic turnover of heme-copper oxygen reductases, several radicals have been reported, however, their identities and relevance remain elusive. Wilson et al. studied bC*c*O using ascorbate as the reductant and catalytic amounts of Cyt *c* as the mediator to create multiple turnover conditions and reported an 8 G wide radical at $g\approx2$ that amounted to as much as 10% of the enzyme concentration [21]. When they reduced the enzyme with excess Cyt *c* passed down a Sephadex G-25 column to remove the ascorbate, the magnitude of the radical signal decreased to ~1% of the enzyme concentration, but they were unable to determine if the residual signal resulted from some ascorbate, which remained bound to Cyt *c*, or a protein-based radical, thus motivating the need for additional studies. The formation of radicals in the reaction of oxygen with the MV bovine enzyme was reported by Babcock and coworkers in a radioactive iodide trapping study in which they identified a radical on the modified tyrosine, Tyr-244, although the population of the radical was very low (<1% mole fraction of the **P** intermediate) [12]. No direct spectroscopic evidence for the radical was reported.

Wiertz et al. reported the presence of two radicals in the reaction of oxygen with ascorbate-reduced aa_3 C*c*O from *Paracoccus denitrificans* (PdC*c*O) [11]. The first radical species, present from 83 μs to ~1 ms with maximum population at 355 μs, was assigned as a tryptophanyl radical located on W272 (PdC*c*O numbering, W236 in bC*c*O), based on simulations of Q-band data. A second unidentified, narrow radical existed from 83 μs through 6 ms and was termed the "6 ms radical." The radical was 8 G wide with subtle hyperfine couplings. It accounted for ~0.5% of the enzyme concentration and was assigned *g*-values of 2.0022, 1.9965 and 1.9994. The authors suggested the source to be a "main-chain radical" but concluded that its identity and functionality could not be determined. Radicals with similar features in X-band spectra were reported in the bo_3 quinol oxidase from *E. coli* [13]. Neither the locations of the radicals nor their role in catalysis could be determined and their formation could not be correlated with oxygen intermediates postulated during the catalytic cycle.

The need to clearly identify and understand the radicals formed under catalytic conditions motivated this study of radicals formed in the oxygen reaction with fully reduced bC*c*O, using rapid freeze-quench (RFQ) trapping and multi-frequency EPR analysis. Fig. 3 shows X-band CW-EPR spectra for the reaction of ascorbate-reduced bC*c*O with oxygen saturated buffer, freeze-quenched at 50, 150, 1000, and 6000 μs. A narrow radical with a peak-to-trough linewidth of 9 G, superimposed on the spectral features of cupric Cu_A, was detected. The isolated Cu_A^{2+} signal is seen in the RFQ resting C*c*O sample (Fig. 3f) and can be simulated with the parameters, $g_x=1.99$, $g_y=2.02$, and $g_z=2.18$, consistent with reported values [22–24]. The origin of the feature at ~3360 G in the RFQ sample is unknown but it does not interfere with our analysis of the signal at $g\sim2.005$. No new radical signals were generated when resting bC*c*O and BSA were individually mixed with buffer and freeze-quenched demonstrating that the narrow radical was not formed due to passing a non-specific protein solution through the RFQ device. A remarkable feature of the data is the persistence of the narrow radical through 6000 μs, indicating extraordinary stability. High frequency pulsed-EPR (D-band) revealed a powder pattern consistent with approximate axial symmetry that could be simulated with $g_x=2.0068$, $g_y=2.0066$, and $g_z=2.0023$ (Table 1) [25].

To determine if radicals could be generated during multiple turnover conditions, we prepared hand-quenched samples in which O_2-saturated buffer was mixed with bC*c*O reduced with ascorbate and a trace amount of Cyt *c* and allowed to turn over for several minutes. An accumulation of a relatively stable radical species was detected by X-band CW-EPR (Fig. 3e) The signal-to-noise is higher in the multiple-turnover sample, which is a frozen liquid, compared to the frozen powders generated by the RFQ device.

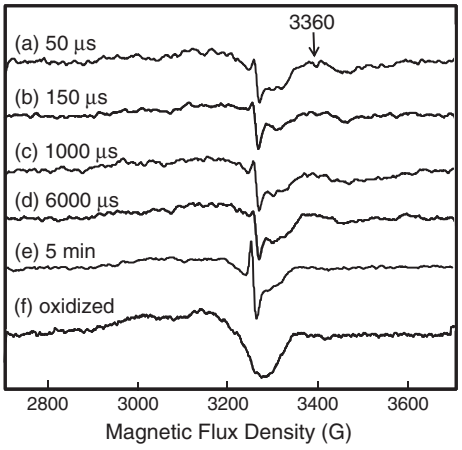

Fig. 3. The X-band EPR spectra of the products of the reaction of oxygen with bovine C*c*O rapidly freeze quenched at several time points following the initiation of the reaction in the presence of ascorbate. The 55 μM samples of bovine C*c*O buffered with 0.2 M sodium phosphate at pH 7.4 containing 0.2% w/v n-decyl-β-D-maltoside (DM) were reduced with 10 mM ascorbate and catalytic amounts of Cyt *c* under Ar and mixed with O_2-saturated buffer. They were freeze quenched at 50 (a), 150 (b), 1000 (c) and 6000 (d) μs after the initiation of the reaction in a rapid mixer. In (e) the oxygen saturated buffer was hand mixed with 100 μM bovine C*c*O with 10 mM ascorbate and catalytic amounts of Cyt *c* and frozen after 5 min of incubation. As a reference the Cu_A spectrum from the oxidized C*c*O is shown in (f). The EPR spectra were measured at 77 K with a microwave power of 1 mW, a microwave frequency of 9.1 GHz and a modulation amplitude of 3.2 G.

Table 1
The *g*-tensor values of the various species. CcO_{red} and CcO_{ox} represent the fully reduced and fully oxidized bC*c*O, respectively. Reaction times are not indicated in the reactions of the fully reduced enzyme with O_2 as the reactions were quenched at several different times.

Species	Linewidth at X-band[a]	g_x	g_y	g_z	Conditions
Ascorbyl	9 G	2.0068	2.0066	2.0023	$CcO_{red} + O_2$
$SO_2^{-\bullet}$	11 G	2.0089	2.0052	2.0017	$CcO_{red} + O_2$
Tyr-244	12 G	2.0059	2.0051	2.0017	$CcO_{ox} + H_2O_2$ (60 s)
Tyr-129	46 G	2.0072	2.0041	2.0023	$CcO_{ox} + H_2O_2$ (60 s)
Peroxyl	16 G	2.03[b]	2.0079	2.0015	$CcO_{ox} + H_2O_2$ (50 μs)
Tyr-129	46 G	2.0072	2.0036	2.0016	$CcO_{ox} + H_2O_2$ (50 μs)

[a] Peak-to-trough linewidth of the most prominent spectral feature in the X-band spectrum.
[b] A Gaussian distribution of 0.014 full width half height in g_x is used in simulations.

The isotropic *g*-value calculated from the trace of the *g*-tensor obtained in the D-band data matches values reported for the ascorbyl radical at room temperature, $g = 2.0052$ [26]. To assess the possible assignment of the radical as an ascorbyl radical, experiments were carried out with isotopically labeled ascorbate. Hand quenched and RFQ samples were prepared with L-[1-^{13}C]-ascorbic acid. Lowering the power to 0.3 mW and narrowing the field sweep to 50 G allowed for resolution of the ascorbyl radical with minimal contributions from Cu_A^{2+} (Fig. 4). A splitting from the ^{13}C nucleus is observed in the spectrum (Fig. 4b) which arises from a hyperfine coupling consistent with that observed previously for isotopically labeled ascorbyl radicals [26]. The linewidth of the natural abundance ascorbyl radical is remarkably narrow, measuring 9 G peak-to-peak, yet unresolved hyperfine splittings broaden the edges of the signal. These spectra are well-simulated as described previously confirming the assignment of the ascorbyl radical [25].

During the catalytic reaction, Cyt *c* acts as the electron mediator between ascorbate and the enzyme, i.e.

$$\text{Cyt } c^{3+} + \text{AsH}^- \rightarrow \text{Cyt } c^{2+} + \text{As}^{\bullet -} + \text{H}^+ \quad (2)$$

$$4\text{Cyt } c^{2+} + CcO_{ox} \rightarrow 4\text{Cyt } c^{3+} + CcO_{red} \quad (3)$$

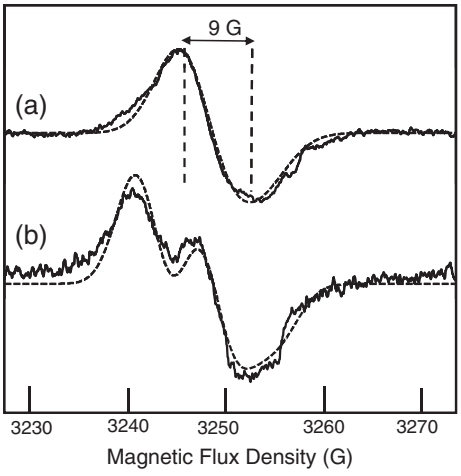

Fig. 4. The X-band EPR spectra of the freeze quenched products of the reaction of oxygen with bovine C*c*O initiated by hand mixing and incubated for 5 min in the presence of natural abundance and isotopically labeled ascorbate. (a) reduction by 10 mM L-[^{12}C] Ascorbate; (b) 10 mM L-[1-^{13}C] Ascorbate. The initial bC*c*O concentration was 100 μM buffered with 0.2 M sodium phosphate at pH 7.4 containing 0.2% w/v DM. The EPR conditions were the same as in Fig. 3, except the microwave power was 0.3 mW. The simulations (dotted lines) were done with the following parameters. (a) *g*-values: 2.0068, 2.0066, 2.0023; isotropic spin ½ (proton) hyperfine coupling values $A_{iso} = 1.76, 0.07, 0.19, 0.19$ (in Gauss). (b) The same parameters as in (a) with the addition of a spin ½ isotropic hyperfine coupling A_{iso} of 6.54 G (corresponding to ^{13}C).

where AsH^- and $\text{As}^{\bullet -}$ are the reduced and the radical forms of ascorbate, respectively, and CcO_{ox} and CcO_{red} represent the oxidized and reduced form of C*c*O, respectively. To obtain insights as to the origin of the ascorbyl radical and its relationship to the one-electron reduction of Cyt *c*, ratios of 1:1 or 20:1 Cyt *c* to reductant were prepared in and frozen within 5 min. Surprisingly, we found that no radicals accumulated in these experiments in the absence of C*c*O. Under our pH 7.4 conditions, the protonated form of ascorbate (AsH^-) is the major form present, although it was reported that the dianion (As^{2-}) is a much better reductant [27]. In addition, it has been shown that the ascorbyl radical is also a better reductant than AsH^- [28], i.e.

$$\text{As}^{\bullet -} + \text{Cyt } c^{3+} \rightarrow \text{Cyt } c^{2+} + \text{As} \quad (4)$$

where As represents the fully oxidized form of ascorbate. Furthermore ascorbyl radicals can decay through dismutation [28]:

$$2\text{As}^{\bullet -} + \text{H}^+ \rightarrow \text{AsH}^- + \text{As} \quad (5)$$

Therefore, the radicals would be expected to be short-lived.

One possibility to account for the absence of ascorbyl radicals with Cyt *c* alone, in contrast to their existence in the presence of bC*c*O, is that with Cyt *c* alone, the ascorbyl radical formed in Eq. (2) serves as a reductant of Cyt *c* (Eq. (4)) thereby generating the diamagnetic dehydroascorbate (As), and thus no radical signal is observed. However, in the presence of bC*c*O, when the Cyt *c* is bound to bC*c*O it is possible that it cannot be reduced by the ascorbyl radical. Although surprising, it has been noted that the ascorbyl radical will not reduce cytochrome b_5 and this has been attributed to the extent of heme exposure [29], and charged groups near the electron transfer sites [30]. When Cyt *c* is bound to C*c*O the solvent exposure is very different, possibly preventing reduction by the ascorbyl radical. Another possibility is that the ascorbyl radical formed in the Eq. (2) reaction is stabilized by binding to bC*c*O preventing the reactions in Eq. (4) or (5) from occurring. Finally, the ascorbyl radical could be formed by serving as a spin trap for radicals possibly generated in the enzyme during turnover (vide infra). Current experiments are in progress in our laboratory to explore these possibilities.

The presence of the ascorbyl radical could interfere with the observation of catalytically relevant radical species; thus, to eliminate the presence of ascorbate, in a new series of experiments, minimal dithionite was used to reduce the enzyme. A narrow (11 G linewidth) radical signal was detected in the reaction of the enzyme freeze quenched from 50 to 6000 μs as shown in Fig. 5. Upon annealing for one minute at 298 K the narrow radical signal disappeared and only the EPR spectrum of Cu_A remained (Spectrum d in Fig. 5). To determine if the radical was a reaction product of dithionite, the reaction of dithionite with both redox active and non-redox active proteins (myoglobin and bovine serum albumin) was rapidly freeze quenched. The same narrow radical signal in the X-band EPR spectrum was formed [25].

Dithionite exists in an equilibrium with radical products:

$$S_2O_4^{2-} \leftrightarrows 2SO_2^{\bullet -} \quad (6)$$

Furthermore, it has been shown that $SO_2^{\bullet -}$ is the most reactive form of dithionite during the reduction of C*c*O [31]. To further characterize the radical species, D-band spectra of the samples were measured which allowed for the determination of the *g* tensor values of g_x, g_y and g_z of 2.0089, 2.0052 and 2.0017, respectively (Table 1). The isotropic *g* value of 2.0053 calculated from these data is in good agreement with the literature value for the $SO_2^{\bullet -}$ radical generated by dithionite [32,33], confirming that the radical originated from the reductant rather than from bC*c*O. The presence of spurious ascorbate and dithionite radicals under turnover conditions demonstrates that great care must be taken when searching for C*c*O-based radicals.

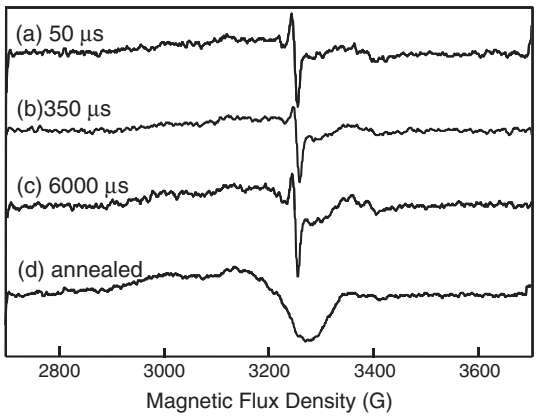

Fig. 5. The X-band EPR spectra of the products of the reaction of oxygen with bC*c*O (100 μM) rapidly freeze quenched at several time points following the initiation of the reaction in the presence of dithionite. The samples of bC*c*O were reduced with 1.5 mM dithionite under Ar and mixed with O_2-saturated buffer. They were freeze quenched at 50 (a), 350 (b) and 6000 (c) μs after the initiation of the reaction in a rapid mixer. In (d) the 350 μs sample was annealed for 1 min at 298 K and the refrozen to 77 K. The solution and EPR conditions were the same as in Fig. 3.

When contributions from ascorbate- or dithionite- based radicals and that from Cu_A are subtracted from our spectra, we do not detect the presence of enzyme-based radicals in our EPR spectra of the RFQ trapped products of the reaction of the fully-reduced bovine enzyme with oxygen. Although the de Vries group used ascorbate as the reductant of bacterial oxidases, their radical spectra do not have the same characteristics of the ascorbyl radicals as that which we detected [11]. Instead, they detected a tryptophanyl radical and an unknown radical at 6 ms after the initiation of the reaction that has different *g* tensor values ($g_{x,y,z}$ = 2.0022, 1.9965, 1.9994) from the ascorbyl radical detected here (see Table 1) [11]. This suggests that there may be differences in the catalytic reaction in the mammalian enzyme in comparison to that in the bacterial enzymes. For example, it is possible that, for the fully reduced enzyme, in which all four electrons needed to reduce oxygen are readily available in the metal centers, the kinetics in the mammalian system may be faster than in the bacterial system, thus preventing the detection of the radical intermediates in the former even under ultrafast RFQ conditions. It is also possible that the electron donation from (and radical formation on) an amino acid is unnecessary in the robust mammalian chemistry but is necessary in the bacterial enzymes to assure rapid reduction of the oxygen and prevent release of reactive oxygen species. Additional experiments are needed to clarify these issues.

3.2. Radical formation in the reactions with hydrogen peroxide

Hydrogen peroxide (H_2O_2) treatment of oxidized C*c*O is a well-established method for generating radicals in the enzyme as a surrogate for those generated in the **P** intermediates during the catalytic reaction with O_2 [34–38]. In the catalytic reaction, **P** intermediates can be formed under two different conditions: when 4 electrons are available from the metal redox centers, an intermediate referred to as $\mathbf{P_R}$ is formed (the subscript **R** represents fully reduced); and when only 2 electrons are available (one each from heme a_3 and Cu_B, while heme *a* and Cu_A remain oxidized) ($\mathbf{P_M}$) is formed (the subscript **M** refers to the mixed valence (MV) form of the enzyme). Under physiological conditions it is thought that $\mathbf{P_M}$ precedes $\mathbf{P_R}$ in the reaction cycle as shown in Fig. 2. An analog of $\mathbf{P_M}$, referred to as $\mathbf{P_H}$ is formed by the reaction of the oxidized enzyme with H_2O_2 at alkaline pH. Electronically, $\mathbf{P_H}$ is similar to $\mathbf{P_M}$ formed in the reaction of oxygen with MV C*c*O, in which only two reducing equivalents are available from the metal centers, in that H_2O_2 also provides two electrons. Indeed, the optical absorption difference spectrum (with respect to the fully oxidized enzyme) of $\mathbf{P_H}$ has a band at 607 nm, just as in $\mathbf{P_M}$ [5,39–41] and amino acid-based radicals are associated with the formation of $\mathbf{P_H}$ [38]. Another ferryl species, termed **F•**, forms by reacting C*c*O with H_2O_2 at weakly acidic pH (6.0). It is assigned as an intermediate with an amino acid based radical and an optical transition at ~575 nm [38,42] similar to that of the catalytic intermediate, **F** (Fig. 2), which, however, is not associated with a radical.

The EPR identification of the radicals formed by H_2O_2 treatment in both PdC*c*O and bC*c*O and their correlation with specific intermediates formed under oxygen turnover conditions have been controversial. In PdC*c*O, a radical was reported to form on Tyr-167 (equivalent to Tyr-129 in bC*c*O) [37,42]. However, in bC*c*O, a wide (peak-to-trough linewidth = 45 G) and a narrow (peak-to-trough linewidth = 12 G) radical were detected by X-band EPR in the reaction with H_2O_2 [34] and were attributed to a tryptophan cation radical (either Trp-126 or Trp-236) and a radical which is the product of a side reaction, respectively [38,43]. In a further comparative study of the data, it was suggested that local interactions could modulate the lineshapes and in bC*c*O the wide radical was on Tyr-129 rather than on a Trp residue [44]. Spectroscopic evidence for radical formation on Tyr-244 in bC*c*O or its equivalent in PdC*c*O has not been reported, despite its potential importance in the catalytic mechanism.

To determine the mechanism of the reaction of H_2O_2 with bovine C*c*O, we used our RFQ system to trap potential radicals within 50 μs [16]. To help guide the interpretation of the data, samples of the fully oxidized enzyme were hand mixed with 5-fold excess of H_2O_2 and frozen within one minute for EPR analysis. As may be seen in Fig. 6, a narrow signal with a width of 12 G, and a broad signal with a width of 46 G, are present in the X-band EPR spectra. The broad resonance is strongest at pH 6 and the narrow resonance is strongest at pH 8. Analysis of X-band and D-band data from hand mixed samples have allowed for the assignment of the narrow line to a radical on Tyr-244 and the broad line to a radical residing on Tyr-129 (M. A. Yu et al. to be submitted). The *g*-tensor values for these radical species are listed in Table 1.

When the reaction was initiated with the RFQ device, a new EPR active species was detected in the X-band spectrum. As evident in Fig. 7, the same signal was detected at both pH 6 and pH 8. We measured the D-band spectrum (Fig. 8) to resolve the *g* tensor values for this radical and found contributions from 2 different radical species. The major component can be simulated using g_x, g_y and g_z tensor values of ~2.03, 2.0079 and 2.0015, respectively, and can be assigned to a peroxyl species. The determination of the precise value

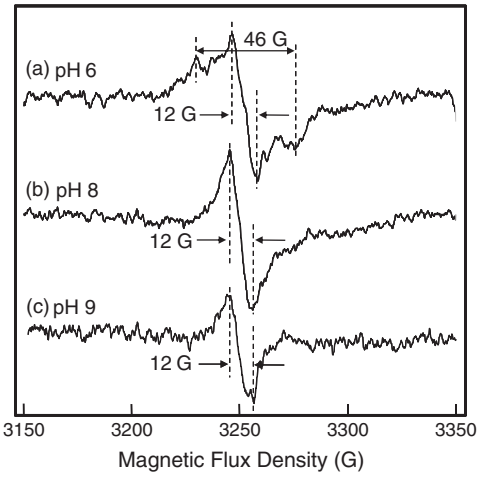

Fig. 6. X-band CW-EPR spectra of species formed in the reaction of H_2O_2 with bC*c*O at pH 6 (a), 8 (b) and 9 (c). The bC*c*O (70 μM) was reacted with 500 μM H_2O_2 and quenched at 60 s in liquid nitrogen. The buffers were: 200 mM BIS–TRIS + 0.2% w/v DM at pH 6, 200 mM HEPES + 0.2% w/v DM at pH 8, and 200 mM CHES + 0.2% w/v DM at pH 9. Spectra of the resting enzyme at pH 6 and 8 were subtracted to remove contributions from Cu_A. The EPR conditions were the same as in Fig. 3.

of g_x is hindered by a large distribution in this parameter (as has been observed in previous studies of peroxyl radicals [45]) and by underlying copper signals. Double integration of the X-band spectrum (Fig. 7) indicates that the population of the peroxyl radical accounts for ~15% of the enzyme concentration. Peroxyl species have been reported by the treatment of H_2O_2 in several heme proteins [46] and is believed to proceed by the reaction of O_2 with an amino acid based radical:

$$R^{\bullet} + O_2 \rightarrow R-O-O^{\bullet} \quad (7)$$

To test this mechanism we carried out the reaction in the presence and absence of O_2. In the absence of O_2 the intensity of the second radical species (designated by the asterisk in Fig. 8c) is much stronger relative to the peroxyl radical when compared to the spectrum obtained in the presence of O_2 (Fig. 8a). Similar behavior was reported in myoglobin by Kelman et al. [47], who found that the peroxyl radical was present only in aerobic samples and in its absence a radical resided on an amino acid. When both samples in Fig. 8 were annealed to 200 K for 30 min only the peroxyl species remained in the spectrum.

Peroxyl radicals (R–O–O•) have been well characterized in myoglobins and hemoglobins treated with peroxide [46]. These radicals all have a central feature at g~2.00 and a component of variable intensity at g_x~2.03 [46]. Winfield and co-workers first noted that oxygenation of free radicals in myoglobins treated with peroxide produced a feature at 2.03 [48,49] and this feature was definitively assigned to a peroxyl radical through spin-trapping measurements [50]. Konovalova et al. studied the g-anisotropy of peroxyl radicals formed on pure tyrosine, tryptophan, and histidine adducts at three different frequencies [45]. They reported g-tensor values for Tyr-OO•, Trp-OO• and His-OO• as summarized in Table 2. The g_y component varies the most for the different parent amino acids. The g-values reported here for the 16 G radical (peak-to-trough linewidth of the most prominent spectral feature) in C*c*O are g_x~2.03, $g_y = 2.0079$, and $g_z = 2.0015$, which is most consistent with tyrosine peroxyl species (Tyr-OO•). However, we cannot rule out that the peroxyl resides on a tryptophan as it has been reported as the source of the peroxyl in the globins [51–54].

To determine the origin of the second radical species, the annealed spectra were subtracted from the original spectra quenched at 50 μs,

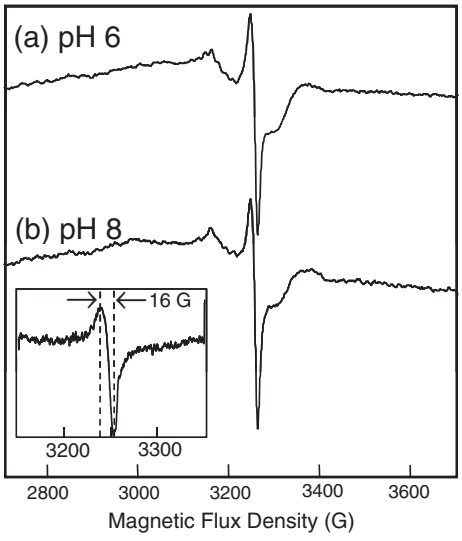

Fig. 7. X-band CW-EPR spectra of the reaction products of H_2O_2 and b*Cc*O trapped via rapid freeze-quench at pH 6 (a) and pH 8 (b). The b*Cc*O (160 μM) was reacted with 2.2 M H_2O_2 and trapped at 50 μs. The buffers were: 200 mM BIS–TRIS + 0.2% w/v DM at pH 6, 200 mM HEPES + 0.2% w/v DM at pH 8. The EPR conditions were the same as in Fig. 3.

and spectrum e in Fig. 8 was obtained. The population of this radical relative to the peroxyl species is between 2 and 10% depending on the presence or absence of O_2. Although the signal to noise ratio is not optimal we were able to extract g tensor values of 2.0072, 2.0036 and 2.0016 for g_x, g_y and g_z, respectively. The g_x component lies in the range of tyrosine radicals ($2.006 < g_x < 2.009$) and effectively rules out tryptophan, cysteine, and histidine radicals. Within the uncertainty of the data, these g-values agree very well with the g-tensor values we obtained in the hand mixing experiments reported in Fig. 6. Thus, we tentatively assign the radical as residing on Tyr-129.

3.3. Mechanism of the H_2O_2 reaction with C*c*O

Based on the data reported above, we postulate the following mechanism for the reaction shown in Fig. 9. In the first step, H_2O_2 reacts with the oxidized enzyme to form a hydroperoxo intermediate. The reaction of H_2O_2 with the heme iron was confirmed as the initial step in the mechanism by experiments in which C*c*O pre-incubated with cyanide failed to produce radical signals under any reaction conditions. Cyanide binds tightly to the Fea_3, which blocks the heme binding site and prevents the formation of the hydroperoxo intermediate and subsequent radical formation. (This experiment also confirmed that no spurious or degradation-induced enzyme radicals were generated by a direct reaction of the H_2O_2 with enzyme amino acids). The hydroperoxo intermediate rapidly leads to a ferryl Compound I species by cleaving the O–O bond by taking one electron from the Fe^{3+} and one from the heme macrocycle resulting in a porphyrin π-cation radical. It has been shown in the past that such an intermediate likely precedes the formation of a radical on an amino acid such as Compound ES in C*c*P and in fact such an intermediate has been detected in some cases[55–57]. This compound I species rapidly accepts an electron from Tyr-244 generating the **P_H** intermediate and a radical on Tyr-244, as we have demonstrated previously (M.A. Yu, to be published). This radical can migrate to Tyr-129 during the formation of the **F•** intermediate. Either or both of these radical species may react with O_2 to form the peroxyl species we detect. At present our data does not allow for the discrimination between these two possibilities or even the possibility that the peroxyl resides on a different residue.

As shown in Fig. 6 when we hand mixed the enzyme with H_2O_2 at pH 8 the dominant intermediate was that assigned as originating from Tyr-244. However, the analysis of the data of the radical species present in the EPR spectra of the RFQ samples indicates that the radical is located on an unmodified tyrosine, based on the hyperfine interactions evident at X-band and g-values measured at D-band, likely Tyr-129. Given that our data is consistent with radical migration between Tyr-244 and Tyr-129, these results may indicate that the peroxyl forms faster on Tyr-244 and thus we detect the remaining tyrosyl radical on Tyr-129.

The difference in the relative amounts of the peroxyl and tyrosyl radicals formed when using O_2 saturated compared to Argon purged buffer in Fig. 8 confirms that the formation of the peroxyl species depends on the presence of O_2. However, a significant population of the peroxyl radical is formed under conditions in which great care was taken to make the samples O_2-free. We attribute the presence of O_2 in these preparations to three possibilities. First, it is well known that trace amounts of metals can lead to the disproportionation of H_2O_2 into O_2 and H_2O [58]. Second, the Compound I formed by the reaction of H_2O_2 with C*c*O could support a catalase type of reaction [59] owing to the high concentrations of H_2O_2 used in the RFQ experiments. This reaction would proceed as follows:

$$H_2O_2 + [Por^{\bullet+}Fe^{4+} = O] \rightarrow H_2O + O_2 + [Por\ Fe^{3+}] \quad (8)$$

Here, [Por•$^+$ Fe^{4+} = O] represents the Compound I porphyrin π-cation radical on heme a_3 and [Por Fe^{3+}] represents the ferric form

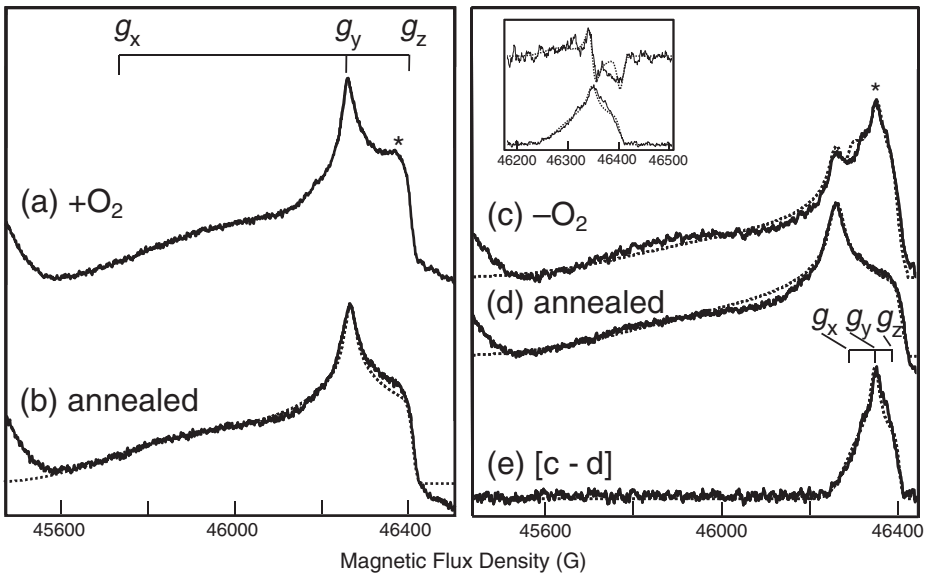

Fig. 8. High-frequency pulsed EPR (D-band) of the reaction products of H_2O_2 and bC*c*O with and without oxygen at pH 8 was measured at 7 K. (a) The bC*c*O (210 μM) in 200 mM O_2 saturated BIS–TRIS + 0.2% w/v DM was reacted with 2.2 M H_2O_2 and trapped at 50 μs. (b) The sample from (a) was annealed at 200 K for 30 min and then reduced to 7 K for the measurement. (c) The bC*c*O (210 μM) in 200 mM O_2-free BIS–TRIS + 0.2% w/v DM was reacted with 2.2 M H_2O_2 and trapped at 50 μs. (d) The sample from (c) was annealed at 200 K for 30 min and then reduced to 7 K for the measurement. (e) The spectrum from (d) was subtracted from that in (c). The inset is an expansion of the derivative and absorption profiles of the spectrum (e). Field swept Hahn echo detected D-band spectra were obtained with the following parameters: temperature, 7 K; repetition rate, 30 Hz; 30 averages per point; 90° pulse, 50 ns; time τ between pulses, 130 ns. The simulations (dotted lines) were done with the following parameters. (b) and (d): $g_x = 2.03$, $g_y = 2.0079$, and $g_z = 2.0015$; Gaussian distribution in $g_x = 0.014$ full width at half height. This distribution precludes a precise determination of g_x. (e) and inset: $g_x = 2.0072$, $g_y = 20{,}036$, and $g_z = 2.0016$; S/N precluded the determination of any hyperfine coupling parameters in these spectra. (c) Simulation was a sum of the simulations from (d) and (e).

of heme a_3. This type of process was invoked by Kelman et al. [47] to account for the observed oxygen isotope distribution of the peroxyl species formed in myoglobin in mixed ^{16}O–^{17}O experiments. Third, X-ray crystallographic structures of the resting C*c*O from bovine [60,61], *Paracoccus denitrificans* [62] and *Rhodobacter sphaeroides* [63] have revealed the presence of electron density between Cu_B and the iron of heme a_3. This has been interpreted as originating from peroxide bridge in the bovine [60,61] and *Paracoccus denitrificans* [62] structures. Redox titration results are consistent with the presence of such a peroxide bridge [15]. Thus, the first step in the reaction of the resting C*c*O with H_2O_2 would be a disproportionation reaction:

$$Fe a_3 - O^- - O^- - Cu_B + H_2O_2 \rightarrow Fe a_3 - OH^- Cu_B - OH^- + O_2 \qquad (9)$$

By this mechanism, the O_2 would be generated within the heme pocket. (Although we have written the product as containing an OH^- ion on both the Fe and Cu_B, the actual ligation states in the oxidized enzyme subsequent to the reaction step in Eq. (9) are not well-established.) Any of these possibilities or a combination of all could generate the O_2 that reacts with the amino acid-based radical to form the peroxyl species.

The experiments reported here show that radicals are rapidly formed (time scale ~50 μs) in the reaction of bC*c*O with H_2O_2 and a subsequent reaction with O_2 generates peroxyl species. In contrast, when the same reaction is initiated by hand mixing the enzyme with H_2O_2 and freeze trapping it on the minutes time scale, the peroxyl intermediate is not detected and instead radicals centered on Tyr-244 and Tyr-129 are identified. With the present data in which the time points of the quenching differ by a factor of 10^6 and the H_2O_2 concentrations are very different, we are unable to reconcile the different observations. Additional experiments are needed spanning the time range to determine the relationship between the early events and the later events. Such experiments will also help to address the question of whether or not peroxyl radicals are involved in the catalytic reaction of the reduced enzyme with O_2.

Table 2
Comparison of the g-tensor values for reported peroxyl radicals on various residues compared to those obtained in the reaction of H_2O_2 with bC*c*O.

Species	g_x	g_y	g_z	Reference
His-OO•	2.03630	2.00690	2.00040	[45]
Trp-OO•	2.03790	2.00375	2.00195	[45]
Tyr-OO•	2.03560	2.00840	2.00250	[45]
Tyr-OO•	2.03	2.0079	2.0015	This work

3.4. Functional implications

The role of radicals in the function of the terminal oxidase superfamily remains controversial. Over the past few years, new radicals have been reported in the reaction of oxygen with the fully reduced bacterial enzymes and have been postulated to play a role in proton translocation [10,11]. Related radicals have not been detected in mammalian C*c*O and instead we have reported that radicals are generated that reside on the reductant used to prepare the reduced forms of the enzyme instead of on the enzyme itself [25]. In the case of ascorbate this is especially intriguing as the radical is only generated when ascorbate is used to reduce bC*c*O with catalytic amounts of Cyt *c*, whereas no radical is generated on the ascorbate when it is used to reduce Cyt *c* alone. Thus, it is possible that the ascorbate is acting as a spin trap, capturing a short-lived radical formed in the mammalian enzyme during turnover. If peroxyl radicals are generated in bC*c*O during the oxygen reaction, as in the H_2O_2 reaction, the radical could migrate to the ascorbate, as is well documented for peroxyl radicals on other proteins [64–66]. Current experiments are planned to test this hypothesis.

When an insufficient number of electrons are available on the metal redox sites to cleave the O – O bond, an additional electron source is needed, which is most plausibly supplied by an amino acid with the concomitant formation of a radical in it, and it is widely believed that the initial radical is formed on Tyr-244 [1]. Our H_2O_2

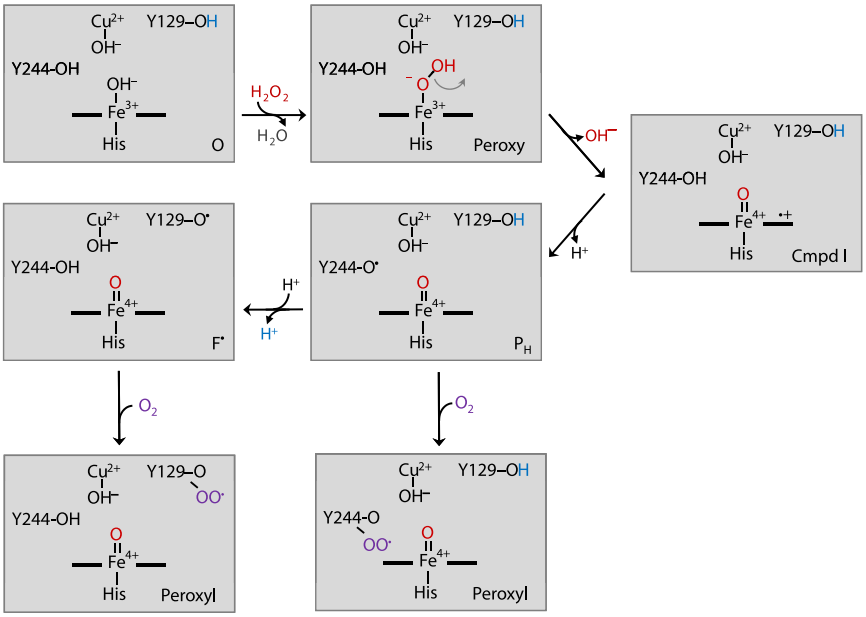

Fig. 9. Schematic pathway for the formation of peroxyl radicals. In this scheme the starting structure is designated as **O** in which an OH^- ligand is on Cu_B and the iron of heme a_3 is 5-coordinate. However, it has been shown that in the resting enzyme, the Cu and the Fe are bridged by a peroxide [60–63]. Thus. the **O** species in the scheme would be formed by the H_2O_2 reduction of the bridged species as shown in Eq. (9). Subsequently, hydroperoxy intermediate is formed that is rapidly converted to a compound I species. The radical on the porphyrin then migrates to Tyr-244 forming a radical on it that is in equilibrium with radical formation on Tyr-129. Either of these two radical species may then react with O_2 to form the peroxyl radical species.

experiments demonstrate that a radical can form on this residue and offer support for this hypothesis. It is less clear if a radical is generated in the case of a fully reduced form of the enzyme when the metal centers can supply an adequate number of electrons to cleave the O – O bond. However, to assure that the reduction process is rapid and thereby preventing the release of reactive oxygen species, transient donation of an electron could still occur with the concomitant generation of an amino acid-based radical.

Another issue concerning the function of the enzyme is whether or not radicals play a role in proton translocation beyond their putative roles in the redox chemistry. In this regard the location of Tyr-129 is particularly interesting. Formation of radicals on this residue has been reported in bacterial oxidases [37,67] and in bCcO as well, as reported here. If the initial radical is formed on Tyr-244, a pathway exists for radical migration to Tyr-129 as may be seen in Fig. 10. This pathway can occur via the interactions between Tyr-244, His-240, Trp-236 to Tyr-129. Thus, the radical, which is initially formed on Tyr-244, may very efficiently migrate to Tyr-129 to form a neutral radical species with the release of a proton. When the radical is located on Tyr-244, introduction of a proton into the catalytic site could raise its redox potential and serve as the driving force for reduction of the radical on Tyr-244 with the concomitant formation of a radical on Tyr-129.

For efficient proton translocation, there needs to be a site at which protons are stored (a proton loading site) from which they can be translocated to the positive side of the membrane when triggered by changes in the metal centers. The proton loading site has been widely postulated to reside in the region of the heme a_3 propionate groups [68] which are bridged by a highly conserved water molecule (molecule a in Fig. 10 is ~2.65 Å from each propionate carboxyl group). This molecule is 2.8 Å from water molecule b which is 3.4 Å from water molecule c which is in H-bonding distance Tyr-129 (Fig. 10). Thus, Tyr-129 may be a key element in the proton loading site by ejecting a proton during radical formation and becoming reprotonated via the water channel upon reduction of the radical. If the residues and water molecules in the loading site region are fully protonated, the released proton would be forced to be ejected toward the positive side of the membrane. Upon reduction of the radical on Tyr-129, the residue would be reprotonated by a proton from the water molecule that is within H-bonding distance as no labile proton groups exist within 6 Å in the direction of the positive side of the membrane. The water molecule would ultimately be reprotonated from protons supplied from the D- or K-channel originating on the negative side of the membrane. Thus, because of its unique location, Tyr-129 becomes an effective proton diode when it switches between a neutral radical and a neutral residue. As such Tyr-129 could play a

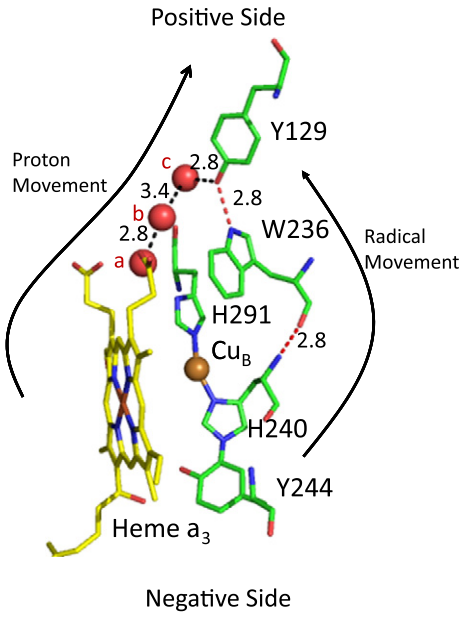

Fig. 10. The structure of the heme a_3–Cu_B binuclear center with its relationship to Tyr-244 and Tyr-129. The red spheres are water molecules that are part of the water cluster near the heme a_3 propionates. These three water molecules directly link the propionate region (water molecule a) to Tyr-129 by the illustrated H-bonding network (black dashed lines). The radical migration between Tyr-244 and Tyr-129 may occur through the linked Y244, H240, W236, Y129 network. The H-bond distances in Å are indicated. The figure was made from PDB ID: 3AG3 with PyMol Molecular Graphics Software (Delano Scientific, LLC).

central role in the regulation of proton translocation, although additional experiments are needed to confirm the postulated directionality.

Acknowledgments

Funding for this work was provided by the National Institutes of Health Grants GM074982 to D.L.R. and GM075920 to G.J.G and the National Science Foundation Grant NSF0956358 to S.-R.Y. M.A.Y. was supported by the Medical Scientist Training Program (GM07288) at Albert Einstein College of Medicine. S.Y. is supported in part by the Grants-in-Aid for Scientific Research 2247012 by the Targeted Protein Research Program, and the Global Center of Excellence program, each provided by the Japanese Ministry of Education, Culture, Sports, Science and Technology.

Appendix A. Supplementary data

Supplementary data to this article can be found online at doi:10.1016/j.bbabio.2011.06.012.

References

[1] I. Belevich, M.I. Verkhovsky, Molecular mechanism of proton translocation by cytochrome c oxidase, Antioxid. Redox Signal. 10 (2008) 1–29.
[2] S. Ferguson-Miller, G.T. Babcock, Heme/copper terminal oxidases, Chem. Rev. 7 (1996) 2889–2907.
[3] R.B. Gennis, Coupled proton and electron transfer reactions in cytochrome oxidase, Front. Biosci. 9 (2004) 581–591.
[4] C. Varotsis, Y. Zhang, E.H. Appelman, G.T. Babcock, Resolution of the reaction sequence during the reduction of O2 by cytochrome oxidase, Proc. Natl. Acad. Sci. U.S.A. 90 (1993) 237–241.
[5] O. Einarsdottir, I. Szundi, Time-resolved optical absorption studies of cytochrome oxidase dynamics, Biochim. Biophys. Acta 1655 (2004) 263–273.
[6] S. Han, S. Takahashi, D.L. Rousseau, Time dependence of the catalytic intermediates in cytochrome c oxidase, J. Biol. Chem. 275 (2000) 1910–1919.
[7] T. Kitagawa, T. Ogura, Time-resolved resonance Raman investigation of oxygen reduction mechanism of bovine cytochrome c oxidase, J. Bioenerg. Biomembr. 30 (1998) 71–79.
[8] D.L. Rousseau, S. Han, Time-resolved resonance Raman spectroscopy of intermediates in cytochrome oxidase, Methods Enzymol. 354 (2002) 351–368.
[9] P. Brzezinski, R.B. Gennis, Cytochrome c oxidase: exciting progress and remaining mysteries, J. Bioenerg. Biomembr. 40 (2008) 521–531.
[10] S. de Vries, The role of the conserved tryptophan272 of the *Paracoccus denitrificans* cytochrome c oxidase in proton pumping, Biochim. Biophys. Acta 1777 (2008) 925–928.
[11] F.G. Wiertz, O.M. Richter, B. Ludwig, S. de Vries, Kinetic resolution of a tryptophan-radical intermediate in the reaction cycle of *Paracoccus denitrificans* cytochrome c oxidase, J. Biol. Chem. 282 (2007) 31580–31591.
[12] D.A. Proshlyakov, M.A. Pressler, C. DeMaso, J.F. Leykam, D.L. DeWitt, G.T. Babcock, Oxygen activation and reduction in respiration: involvement of redox-active Tyrosine 244, Science 290 (2000) 1588–1590.
[13] F.G. Wiertz, O.M. Richter, A.V. Cherepanov, F. MacMillan, B. Ludwig, S. de Vries, An oxo-ferryl tryptophan radical catalytic intermediate in cytochrome c and quinol oxidases trapped by microsecond freeze-hyperquenching (MHQ), FEBS Lett. 575 (2004) 127–130.
[14] S. Yoshikawa, M.G. Choc, M.C. O'Toole, W.S. Caughey, An infrared study of CO binding to heart cytochrome c oxidase and hemoglobin A. Implications re O2 reactions, J. Biol. Chem. 252 (1977) 5498–5508.
[15] M. Mochizuki, H. Aoyama, K. Shinzawa-Itoh, T. Usui, T. Tsukihara, S. Yoshikawa, Quantitative reevaluation of the redox active sites of crystalline bovine heart cytochrome c oxidase, J. Biol. Chem. 274 (1999) 33403–33411.
[16] T. Egawa, J.L. Durand, E.Y. Hayden, D.L. Rousseau, S.R. Yeh, Design and evaluation of a passive alcove-based microfluidic mixer, Anal. Chem. 81 (2009) 1622–1627.
[17] Y. Lin, G.J. Gerfen, D.L. Rousseau, S.R. Yeh, Ultrafast microfluidic mixer and freeze-quenching device, Anal. Chem. 75 (2003) 5381–5386.
[18] V. Krymov, G.J. Gerfen, Analysis of the tuning and operation of reflection resonator EPR spectrometers, J. Magn. Reson. 162 (2003) 466–478.
[19] K. Ranguelova, S. Girotto, G.J. Gerfen, S. Yu, J. Suarez, L. Metlitsky, R.S. Magliozzo, Radical sites in *Mycobacterium tuberculosis* KatG identified using electron paramagnetic resonance spectroscopy, the three-dimensional crystal structure, and electron transfer couplings, J. Biol. Chem. 282 (2007) 6255–6264.
[20] F. Malatesta, G. Antonini, P. Sarti, M. Brunori, Structure and function of a molecular machine: cytochrome c oxidase, Biophys. Chem. 54 (1995) 1–33.
[21] M.T. Wilson, P. Jensen, R. Aasa, B.G. Malmstrom, T. Vanngard, An investigation by e.p.r. and optical spectroscopy of cytochrome oxidase during turnover, Biochem. J. 203 (1982) 483–492.
[22] B.M. Hoffman, J.E. Roberts, M. Swanson, S.H. Speck, E. Margoliash, Copper electron-nuclear double resonance of cytochrome c oxidase, Proc. Natl. Acad. Sci. U.S.A. 77 (1980) 1452–1456.
[23] H. Beinert, D.E. Griffiths, D.C. Wharton, R.H. Sands, Properties of the copper associated with cytochrome oxidase as studied by paramagnetic resonance spectroscopy, J. Biol. Chem. 237 (1962) 2337–2346.
[24] Y. Zhen, B. Schmidt, U.G. Kang, W. Antholine, S. Ferguson-Miller, Mutants of the CuA site in cytochrome c oxidase of *Rhodobacter sphaeroides*: I. Spectral and functional properties, Biochemistry 41 (2002) 2288–2297.
[25] M.A. Yu, T. Egawa, S.R. Yeh, D.L. Rousseau, G.J. Gerfen, EPR characterization of ascorbyl and sulfur dioxide anion radicals trapped during the reaction of bovine cytochrome c oxidase with molecular oxygen, J. Magn. Reson. 203 (2010) 213–219.
[26] G.P. Laroff, R.W. Fessenden, R.H. Schuler, The electron spin resonance spectra of radical intermediates in the oxidation of ascorbic acid and related substances, J. Am. Chem. Soc. 94 (1972) 9062–9073.
[27] A.I. Al-Ayash, M.T. Wilson, The mechanism of reduction of single-site redox proteins by ascorbic acid, Biochem. J. 177 (1979) 641–648.
[28] I. Yamazaki, The reduction of cytochrome c by enzyme-generated ascorbic free radical, J. Biol. Chem. 237 (1962) 224–229.
[29] T.E. Meyer, C.T. Przysiecki, J.A. Watkins, A. Bhattacharyya, R.P. Simondsen, M.A. Cusanovich, G. Tollin, Correlation between rate constant for reduction and redox potential as a basis for systematic investigation of reaction mechanisms of electron transfer proteins, Proc. Natl. Acad. Sci. U.S.A. 80 (1983) 6740–6744.
[30] T. Iyanagi, I. Yamazaki, K.F. Anan, One-electron oxidation–reduction properties of ascorbic acid, Biochimica et Biophysica Acta (BBA)—Bioenergetics 806 (1985) 255–261.
[31] G.D. Jones, M.G. Jones, M.T. Wilson, M. Brunori, A. Colosimo, P. Sarti, Reactions of cytochrome c oxidase with sodium dithionite, Biochem. J. 209 (1983) 175–182.
[32] I. Streeter, A.J. Wain, J. Davis, R.G. Compton, Cathodic reduction of bisulfite and sulfur dioxide in aqueous solutions on copper electrodes: an electrochemical ESR study, J. Phys. Chem. B 109 (2005) 18500–18506.
[33] J. Zhu, K. Petit, O. Colson, S. DeBolt, M.D. Sevilla, Reactions of HS and S* with molecular oxygen, H2S, HS-, and S2': formation of SO2', HSSH', HSS2', and HSS', J. Phys. Chem. 95 (1991) 3676–3681.
[34] M. Fabian, G. Palmer, The interaction of cytochrome oxidase with hydrogen peroxide: the relationship of compounds P and F, Biochemistry 34 (1995) 13802–13810.
[35] S. Junemann, P. Heathcote, P.R. Rich, The reactions of hydrogen peroxide with bovine cytochrome c oxidase, Biochim. Biophys. Acta 1456 (2000) 56–66.
[36] F. MacMillan, K. Budiman, H. Angerer, H. Michel, The role of tryptophan 272 in the *Paracoccus denitrificans* cytochrome c oxidase, FEBS Lett. 580 (2006) 1345–1349.
[37] F. MacMillan, A. Kannt, J. Behr, T. Prisner, H. Michel, Direct evidence for a tyrosine radical in the reaction of cytochrome c oxidase with hydrogen peroxide, Biochemistry 38 (1999) 9179–9184.
[38] P.R. Rich, S.E. Rigby, P. Heathcote, Radicals associated with the catalytic intermediates of bovine cytochrome c oxidase, Biochim. Biophys. Acta 1554 (2002) 137–146.
[39] D.A. Proshlyakov, M.A. Pressler, G.T. Babcock, Dioxygen activation and bond cleavage by mixed-valence cytochrome c oxidase, Proc. Natl. Acad. Sci. U.S.A. 95 (1998) 8020–8025.
[40] D.A. Proshlyakov, T. Ogura, K. Shinzawa-Itoh, S. Yoshikawa, E.H. Appelman, T. Kitagawa, Selective resonance Raman observation of the "607 nm" form generated in the reaction of oxidized cytochrome c oxidase with hydrogen peroxide, J. Biol. Chem. 269 (1994) 29385–29388.
[41] D.A. Proshlyakov, T. Ogura, K. Shinzawa-Itoh, S. Yoshikawa, T. Kitagawa, Resonance Raman/absorption characterization of the oxo intermediates of cytochrome c oxidase generated in its reaction with hydrogen peroxide: pH and H2O2 concentration dependence, Biochemistry 35 (1996) 8580–8586.
[42] K. Budiman, A. Kannt, S. Lyubenova, O.M. Richter, B. Ludwig, H. Michel, F. MacMillan, Tyrosine 167: the origin of the radical species observed in the reaction of cytochrome c oxidase with hydrogen peroxide in *Paracoccus denitrificans*, Biochemistry 43 (2004) 11709–11716.
[43] S.E. Rigby, S. Junemann, P.R. Rich, P. Heathcote, Reaction of bovine cytochrome c oxidase with hydrogen peroxide produces a tryptophan cation radical and a porphyrin cation radical, Biochemistry 39 (2000) 5921–5928.
[44] D.A. Svistunenko, M.T. Wilson, C.E. Cooper, Tryptophan or tyrosine? On the nature of the amino acid radical formed following hydrogen peroxide treatment of cytochrome c oxidase, Biochim. Biophys. Acta 1655 (2004) 372–380.
[45] T.A. Konovalova, L.D. Kispert, J. van Tol, L.-C. Brunel, Multifrequency high-field electron paramagnetic resonance characterization of the peroxyl radical location in horse heart myoglobin oxidized by H2O2, J. Phys. Chem. B 108 (2004) 11820–11826.
[46] D.A. Svistunenko, Reaction of haem containing proteins and enzymes with hydroperoxides: the radical view, Biochim. Biophys. Acta 1707 (2005) 127–155.
[47] D.J. Kelman, J.A. DeGray, R.P. Mason, Reaction of myoglobin with hydrogen peroxide forms a peroxyl radical which oxidizes substrates, J. Biol. Chem. 269 (1994) 7458–7463.
[48] N.K. King, F.D. Looney, M.E. Winfield, Myoglobin free-radicals, Biochim. Biophys. Acta 88 (1964) 235–236.
[49] N.K. King, F.D. Looney, M.E. Winfield, Amino acid free radicals in oxidized metmyoglobin, Biochim. Biophys. Acta 133 (1967) 65–82.
[50] B. Kalyanaraman, C. Mottley, R.P. Mason, A direct electron spin resonance and spin-trapping investigation of peroxyl free radical formation by hematin/hydroperoxide systems, J. Biol. Chem. 258 (1983) 3855–3858.

[51] M.R. Gunther, Probing the free radicals formed in the metmyoglobin–hydrogen peroxide reaction, Free Radic. Biol. Med. 36 (2004) 1345–1354.
[52] M.R. Gunther, R.A. Tschirret-Guth, O.M. Lardinois, P.R. Ortiz de Montellano, Tryptophan-14 is the preferred site of DBNBS spin trapping in the self-peroxidation reaction of sperm whale metmyoglobin with a single equivalent of hydrogen peroxide, Chem. Res. Toxicol. 16 (2003) 652–660.
[53] D.A. Svistunenko, An EPR study of the peroxyl radicals induced by hydrogen peroxide in the haem proteins, Biochim. Biophys. Acta 1546 (2001) 365–378.
[54] P.K. Witting, A.G. Mauk, Reaction of human myoglobin and H2O2. Electron transfer between tyrosine 103 phenoxyl radical and cysteine 110 yields a protein-thiyl radical, J. Biol. Chem. 276 (2001) 16540–16547.
[55] A.N. Hiner, E.L. Raven, R.N. Thorneley, F. Garcia-Canovas, J.N. Rodriguez-Lopez, Mechanisms of compound I formation in heme peroxidases, J. Inorg. Biochem. 91 (2002) 27–34.
[56] P.R.O. Montellano, Catalytic sites of hemoprotein peroxidases, Annu. Rev. Pharmacol. Toxicol. 32 (1992) 89–107.
[57] T.L. Poulos, J. Kraut, The stereochemistry of peroxidase catalysis, J. Biol. Chem. 255 (1980) 8199–8205.
[58] D.W. McKee, Catalytic decomposition of hydrogen peroxide by metals and alloys of the platinum group, J. Catalysis 14 (1969) 355–364.
[59] M. Alfonso-Prieto, X. Biarnes, P. Vidossich, C. Rovira, The molecular mechanism of the catalase reaction, J. Am. Chem. Soc. 131 (2009) 11751–11761.
[60] H. Aoyama, K. Muramoto, K. Shinzawa-Itoh, K. Hirata, E. Yamashita, T. Tsukihara, T. Ogura, S. Yoshikawa, A peroxide bridge between Fe and Cu ions in the O2 reduction site of fully oxidized cytochrome c oxidase could suppress the proton pump, Proc. Natl. Acad. Sci. U.S.A. 106 (2009) 2165–2169.
[61] S. Yoshikawa, K. Shinzawa-Itoh, R. Nakashima, R. Yaono, E. Yamashita, N. Inoue, M. Yao, M.J. Fei, C.P. Libeu, T. Mizushima, H. Yamaguchi, T. Tomizaki, T. Tsukihara, Redox-coupled crystal structural changes in bovine heart cytochrome c oxidase, Science 280 (1998) 1723–1729.
[62] J. Koepke, E. Olkhova, H. Angerer, H. Muller, G. Peng, H. Michel, High resolution crystal structure of *Paracoccus denitrificans* cytochrome c oxidase: new insights into the active site and the proton transfer pathways, Biochim. Biophys. Acta 1787 (2009) 635–645.
[63] L. Qin, C. Hiser, A. Mulichak, R.M. Garavito, S. Ferguson-Miller, Identification of conserved lipid/detergent-binding sites in a high-resolution structure of the membrane protein cytochrome c oxidase, Proc. Natl. Acad. Sci. U.S.A. 103 (2006) 16117–16122.
[64] J.M. Gebicki, T. Nauser, A. Domazou, D. Steinmann, P.L. Bounds, W.H. Koppenol, Reduction of protein radicals by GSH and ascorbate: potential biological significance, Amino Acids 39 (2010) 1131–1137.
[65] J.A. Irwin, H. Ostdal, M.J. Davies, Myoglobin-induced oxidative damage: evidence for radical transfer from oxidized myoglobin to other proteins and antioxidants, Arch. Biochem. Biophys. 362 (1999) 94–104.
[66] C. von Sonntag, H.-P. Schuchmann, The elucidation of peroxyl radical reactions in aqueous solution with the help of radiation-chemical methods, Angewandte Chemie International Edition in English, 30, 1991, pp. 1229–1253.
[67] I. von der Hocht, J.H. van Wonderen, F. Hilbers, H. Angerer, F. Macmillan, H. Michel, Interconversions of P and F intermediates of cytochrome c oxidase from *Paracoccus denitrificans*, Proc. Natl. Acad. Sci. U.S.A. 108 (2011) 3964–3969.
[68] H.J. Lee, L. Ojemyr, A. Vakkasoglu, P. Brzezinski, R.B. Gennis, Properties of Arg481 mutants of the aa3-type cytochrome c oxidase from *Rhodobacter sphaeroides* suggest that neither R481 nor the nearby D-propionate of heme a3 is likely to be the proton loading site of the proton pump, Biochemistry 48 (2009) 7123–7131.